Separating dipole and quadrupole contributions to single photon double ionization

S. Grundmann,[1,*] F. Trinter,[1] A. W. Bray,[2] S. Eckart,[1] J. Rist,[1] G. Kastirke,[1] D. Metz,[1] S. Klumpp,[3] J. Viefhaus,[4] L. Ph. H. Schmidt,[1] J. B. Williams,[5] R. Dörner,[1] T. Jahnke,[1] M. S. Schöffler,[1] and A. S. Kheifets[2,†]

[1] *Institut für Kernphysik, Goethe-Universität, 60438 Frankfurt, Germany*
[2] *Research School of Physics, Australian National University, Canberra ACT 2601, Australia*
[3] *FS-FLASH-D, Deutsches Elektronen-Synchrotron (DESY), 22607 Hamburg, Germany*
[4] *Helmholtz-Zentrum, 14109 Berlin, Germany*
[5] *Department of Physics, University of Nevada, Reno, NV 89557, USA*

(Dated: February 28, 2018)

We performed a kinematically complete measurement of photo-double-ionization of helium by a single 1100 eV photon. By exploiting dipole selection rules in the two electron continuum state, we observed the angular emission pattern of electrons originating from a pure quadrupole transition. Our fully differential data and companion ab initio non-perturbative theory shows the separation of dipole and quadrupole contributions to photo-double-ionization and provide new insight into the nature of the quasifree mechanism.

The interaction of photons with atoms and molecules is dominated by electronic dipole transitions due to the photon spin. Any transfer of additional orbital angular momentum arises from the photon's linear momentum $\mathbf{k}_\gamma$ and is consequently supressed for low photon energies. Whenever a transition leads to the continuum, i.e., to the ejection of one or more electrons, the angular momentum becomes observable in the electron angular distributions. These angular distributions result from a coherent superposition of the different multipole contributions, as the various angular momentum states of a free particle are energetically degenerate. In most cases, however, the angular distributions are, due to the dominance of the dipole contribution, only slightly modified by the interference term between the quadrupole and the dipole part. The quadrupole transition amplitude alone has not been directly observed so far.

In the present work we succeeded to experimentally isolate the quadrupole contribution to photo-double-ionization (PDI) and visualize a pure quadrupole pattern in the angular distribution of electrons emitted from a helium atom (Fig. 1). The quadrupole contribution to a photoionization process can be accessed in cases where the dominating dipole contribution is strongly supressed [1]. For the case of double ionization, the selection rules for the two-electron continuum, which have been presented in detail in 1995 [2], can be exploited. The most prominent of these selection rules states that for two electrons of opposite spin the electron pair wave function vanishes for total angular momentum $l{=}\hbar$ and $\mathbf{k_a} = -\mathbf{k_b}$ (where $\mathbf{k_{a,b}}$ are the momentum vectors of electrons a and b). As a result, it is not possible in dipole transitions to emit two electrons from the helium ground state with equal energy back-to-back. At moderate photon energies, this strict dipole selection rule leads to a node in the electron angular distributions for the PDI of He, which has been observed already in the pioneering experiment by [3] and confirmed many times by later work (e.g. [4]). This selection rule holds true only for the $l{=}\hbar$ component of the two-electron wave function. Therefore, the quadrupole components can be observed directly by selecting electrons pairs with opposite momentum of equal magnitude ($\mathbf{k_a} = -\mathbf{k_b}$). This is the approach we have used to isolate the quadrupole distribution shown in Figure 1. In the remainder of this paper, we will first give a brief outline of the experiment and the ab initio theory and then discuss in more detail how the dipole and quadrupole contributions separate in fully differential cross sections of which Figure 1 is a special case.

We used a COLTRIMS reaction microscope (Cold Target Recoil Ion Momentum Spectroscopy [5–7]) and intersected a cold supersonic helium gas jet with a synchrotron beam of 1100 eV circularly polarized photons from beamline P04 at PETRA III (DESY, Hamburg [8]). Electrons and ions were guided by a weak electric field (20.1 V/cm) towards two time- and position-sensitive detectors [9, 10]. Additionally, a strong magnetic field (40 Gauss) was applied in order to confine the high energetic electrons inside the spectrometer. An electrostatic lens and a drift tube of 80 cm length were used on the ion arm of the spectrometer to increase the momentum resolution. The high photon flux of beamline P04 combined with a dense target ($\approx 3{\cdot}10^{11}$ atoms/cm^2) lead to approx. 10 million coincidently measure double ionization events. The experimental results are compared to ab-initio non-perturbative calculations using the convergent close-coupling (CCC) technique. This technique has already shown its utility in identifying various mechanisms behind helium PDI at high photon energies [11, 12].

In our experiment, the momenta of all reaction products are measured in coincidence. In case of PDI, energy and momentum conservation reduce the nine momentum components of the three measured particles to five independent variables. Together with cylinder symmetry of the circularly polarized light, this makes the fully differential cross section fourfold. For an overview, we integrate over some of the observables and inspect singly and doubly differential cross sections.

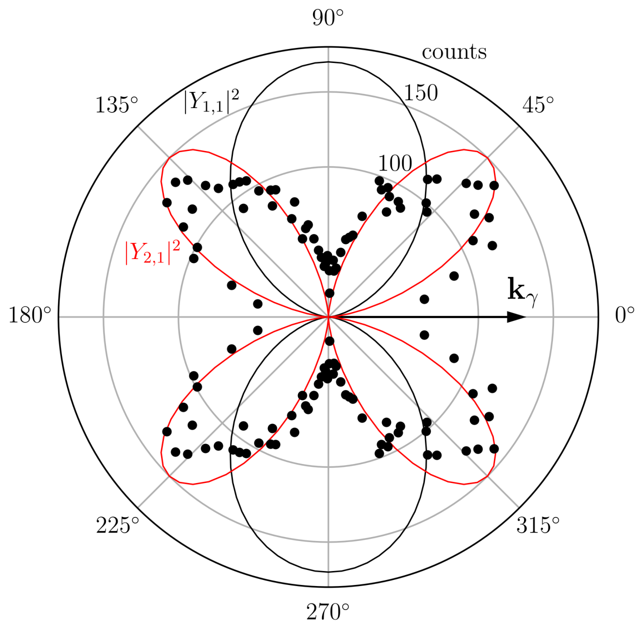

FIG. 1. Angular distribution of one of the electrons from photo-double-ionization of He by a single 1100 eV circularly polarized photon. The light propagation axis is horizontal ($\mathbf{k}_\gamma$). Data points: electrons of equal energy ($\Delta E = 0.5 \pm 0.1$) emitted back-to-back ($\Delta\vartheta = 180 \pm 20°$). For this selection, dipole contributions to the cross section vanish due to selection rules. Black line: dipole distribution ($|Y_{l=1,m=1}|^2$, not inter-normalized), red line: expected quadrupole distribution (($|Y_{l=2,m=1}|^2$).

In Figure 2 we depict the energy sharing between the two electrons $\Delta E = \frac{E_a - E_b}{E_a + E_b}$ and the relative emission angle $\Delta\vartheta$ between both electrons, integrating over all other observables. The single differential cross section $\frac{d\sigma}{d\Delta E}$ for all electron pairs (Fig. 2a, red line) shows a very deep **U**-shape, highlighting that the most likely energy sharing configuration consists of one electron obtaining most of the photon's energy while only sharing a small fraction of it with the second electron. The dominance of strong unequal energy sharing at this high photon energy is a consequence of the interplay of the two established PDI mechanisms "knock-off", also known as "two-step-one" (TS1), and "shake-off" (SO) [13]. In the case of a quasi-instantaneous removal of the first electron, the second electron cannot relax adiabatically to the singly charged ground state. Instead, it can be that the electron is shaken off to the continuum. For the shake-off, small energy transfer, i.e., a very unequal energy sharing, is strongly favoured. The probability for this process is determined solely by the overlap integral of the initial neutral He and final He^+ continuum wave functions. The knock-off process is characterized by a binary collision event between the two electrons and contributes only to a small fraction of PDI events at 1100 eV photon energy [12]. The binary collision leads to an angle of 90° between the momentum vectors of the outgoing collision partners and arbitrary energy sharing. We plot in Figure 2b the doubly differential cross section $\frac{d^2\sigma(\Delta E, \Delta\vartheta)}{d\Delta E d\vartheta}$ as function of the relative angle between the two electrons $\Delta\vartheta$ for equal energy sharing, i.e., $\Delta E = 0.5$, where SO is strongly suppressed. The distribution is a narrowly peaked at $\pm 90°$ as expected for a violent binary TS1 collision. Additionally, a distinct peak for back-to-back emission is visible, located at $\Delta\vartheta = 180°$. Note that this peak is located at the position of the node enforced by the dipole selection rule. By restricting the measured dataset to electron pairs occurring within this peak we obtain the laboratory frame electron angular distribution shown in Figure 1. This subset of the data is, by virtue of the dipole selection rule, free of any otherwise dominating dipole contribution and Figure 1 directly shows an angular distribution of a quadrupole transition almost free of any dipolar contribution. We employed circularly polarized light in our measurement. Thus, by choosing the photon propagation $\mathbf{k}_\gamma$ as quantization axis, the shape of the dipole distribution is given by the square of the spherical harmonic $Y_{l=1,m=1}$ (black line in Fig. 1). In a quadrupole transition, the additional quantum of (orbital) angular momentum is transferred by coupling the linear momentum $\mathbf{k}_\gamma$ to the electron. Classically, this corresponds to an angular momentum of $\mathbf{k}_\gamma \times \mathbf{r}$ which is directed perpendicularly to the light propagation. Hence it increases the magnitude of l but not the projection m of the angular momentum onto $\mathbf{k}_\gamma$. Therefore, the pure quadrupole contribution yields an angular distribution proportional to $|Y_{l=2,m=1}|^2$ (red line in Fig. 1).

In terms of reaction mechanisms, the back-to-back emission at equal energy sharing is the fingerprint predicted for a route to double ionization termed "quasifree mechanism" (QFM) [14], which is dipole forbidden. In the case of QFM, the nucleus is only a spectator to the photo absorption process receiving no momentum [17, 18]. Instead, the two electrons balance each others' momentum. Our experiment confirms the existence of these ions with close to zero momentum which have been confirmed first in [15] (not shown). The probability of such events can be recognized from the black line in Figure 2a, which shows the energy sharing distribution of electrons being emitted back-to-back, i.e., $\frac{d^2\sigma(\Delta E, \Delta\vartheta)}{d\Delta E d\Delta\vartheta}$ as function of ΔE at $\Delta\vartheta = 180°$. This distribution has a **W**-shape as predicted by theory [14]. (SG: didn't find Colgan Paper yet!)

The most complete picture of the double ionization process is provided by fully differential cross sections (FDCS) $\frac{d^4\sigma(\vartheta_a, \vartheta_b, \Phi_{ab}, \Delta E)}{d\vartheta_a d\vartheta_b d\Phi_{ab} d\Delta E}$. Here $\vartheta_{a,b}$ denotes the polar angles of the two electrons with respect to $\mathbf{k}_\gamma$ and Φ_{ab} labels the difference between the respective azimuthal angle, i.e., the angle around the light propagation axis. We inspect the coplanar geometry where $\mathbf{k}_\gamma$, $\mathbf{k_a}$, and $\mathbf{k_b}$ are all in one plane as $\Phi_{ab} = 0, 180°$.

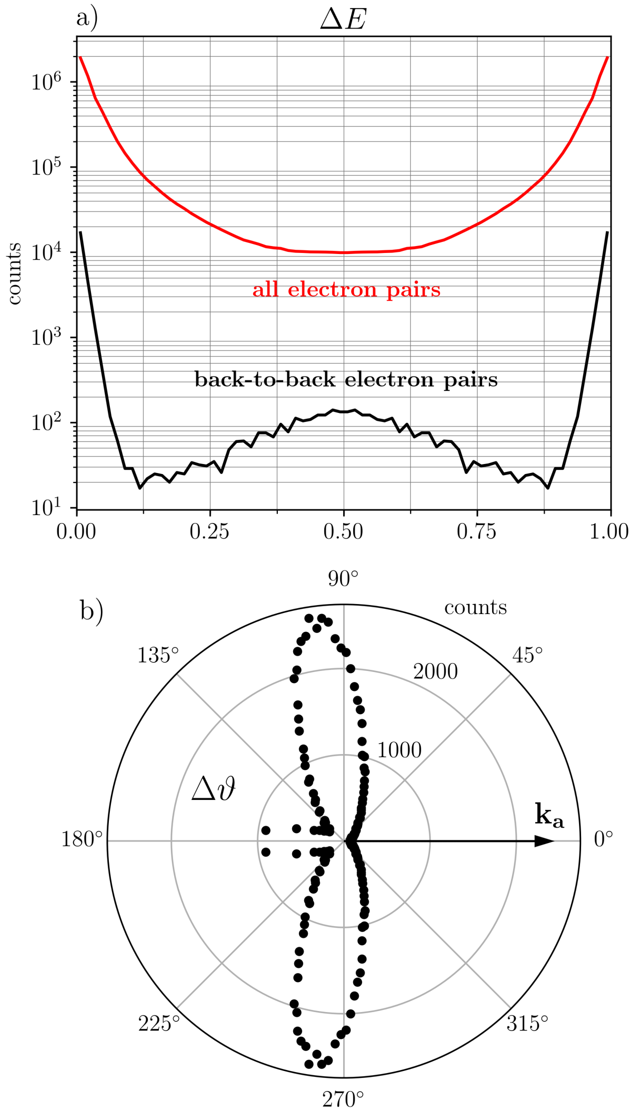

FIG. 2. (a) Red line: single differential cross section for photo-double-ionization of He by a single 1000 eV circularly polarized photon as function of electron energy sharing ΔE. Blue line: double differential cross section for electrons emitted back to back ($\Delta\vartheta = 180 \pm 20°$). (b) Distribution of the relative emission angle $\Delta\vartheta$ between both electrons for equal energy sharing, i.e., double differential cross section $\frac{d^2\sigma(\Delta E,\Delta\vartheta)}{d\Delta E d\Delta\vartheta}$ for $\Delta E = 0.5 \pm 0.1$ as function of $\Delta\vartheta$.

A suitable parametrization of the transition amplitude of He PDI with electrons confined to this coplanar plane has been presented in [16]. This parametrization separates the angular dependence of the transition amplitude from that of the energy dependence and the dipole part A_d from the quadrupole component A_q. While the dipole contribution has the form

$$A_d = f_a \sin\vartheta_a + f_b \sin\vartheta_b \ ,$$

the quadrupole fraction of the amplitude reads as

$$\begin{aligned} A_q &= g_a \cos\vartheta_a \sin\vartheta_a + g_b \cos\vartheta_b \sin\vartheta_b \\ &\quad + g_s [\cos\vartheta_a \sin\vartheta_b + \cos\vartheta_b \sin\vartheta_a] \ . \end{aligned}$$

The dynamic factors f_a, f_b, g_a, g_b, and g_s depend on the electron mutual angle $\Delta\vartheta$ and electron energy sharing ΔE. While their explicit form can be found in [16], it is noteworthy, that the parallel emissions of the two electrons, i.e., $\Delta\vartheta = 0$, is strongly suppressed by these factors. At equal energy sharing, f_a and f_b are identical and

$$A_d \propto \sin\vartheta_a + \sin\vartheta_b = \sin\left(\frac{\vartheta_a + \vartheta_b}{2}\right) \cos\left(\frac{\vartheta_a - \vartheta_b}{2}\right) \ .$$

Consequently, the dipole amplitude in the coplanar plane vanishes, if

$$|\vartheta_a - \vartheta_b| = (2n+1)\pi \text{ or } \vartheta_a + \vartheta_b = 2n\pi \ .$$

In case of back-to-back emission, the first condition is always satisfied. This analysis of the angular factors alone demonstrates how the back-to-back emission with equal energy sharing is dipole-forbidden. Unlike the dipole amplitude however, the quadrupole component allows the back-to-back emission at equal energy sharing, because

$$A_d \propto g_m \cos\vartheta_a \sin\vartheta_a \ ,$$

with $g_a = g_b$ and $g_m = 2g_a + 2g_s$. The squared quadrupole amplitude $|A_q|^2$ possesses the characteristic four-fold symmetry clearly visible in Figure 1.

Figure 3 presents the FDCS restricted to the coplanar geometry and equal energy sharing. Figure 3a shows the dipole contributions to the FDCS as obtained from CCC calculations while Figure 3b shows the results of such calculations for the quadrupole term. We see that due to entirely different symmetries, dipole and quadrupole contributions to the FDCS in the coplanar plane are completely separated. The CCC predictions are in excellent agreement with the experimental results displayed in Figure 3c. The measured distribution can clearly be identified as a superposition of Figures 3a and 3a.

In conclusion, we have separated the quadrupole contribution to photo-double-ionization and identified multiple fingerprints of the QFM electrons in various observables of helium PDI at a high photon energy of 1100 eV. Our measured fully differential cross sections are in excellent agreement with predictions by CCC theory. We find a clean quadrupolar angular distribution in the laboratory frame for electrons that have been emitted back-to-back with equal energy.

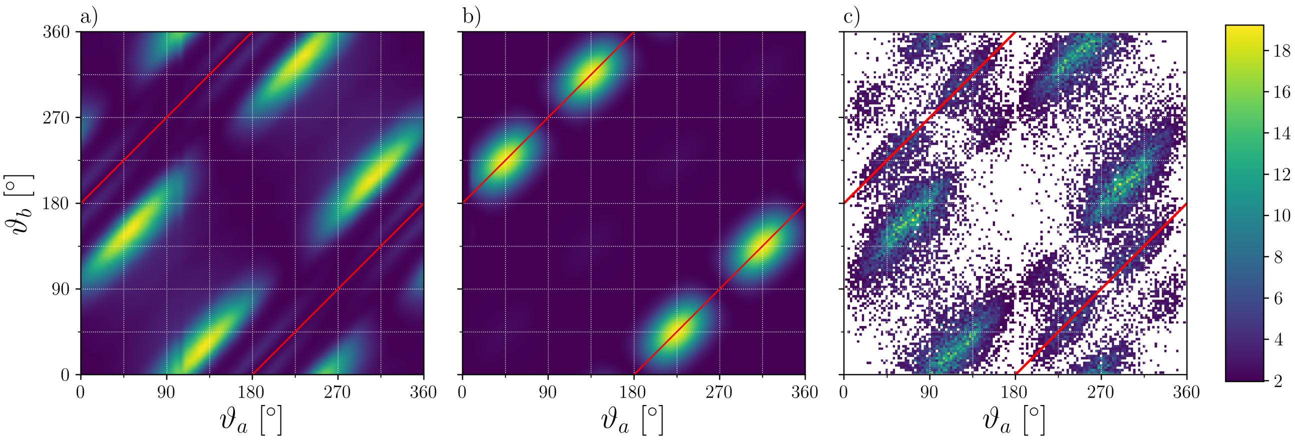

FIG. 3. Fully differential cross section for photo-double-ionization of He by a single 1100 eV circularly polarized photon, $\frac{d^4\sigma(\vartheta_a,\vartheta_b,\Phi_{ab},\Delta_E)}{d\vartheta_a d\vartheta_b d\Phi_{ab} d\Delta_E}$, for coplanar geometry and equal energy sharing. The solid red lines visualize the conditions under which the dipole amplitude vanishes in coplanar geometry. Dipole (a) and quadrupole (b) contributions to the FDCS as obtained from CCC calculations (not inter-normalized). The measured ditribution (c) shows separated dipole and quadrupole contributions with the gates $\Phi_{ab} = 0, 180 \pm 20°$ and $\Delta E = 0.5 \pm 0.1$ and can be identified as the superposition of (a) and (b). $\vartheta_{a,b} = 0°$ corresponds to emission in the photon direction.

AK acknowledges support by the Wilhelm and Else Heraeus Foundation. SK acknowledges the funding of the EUCALL project within the *European Unions Horizon 2020 research and innovation programme* under the grant agreement No. 654220. This work was supported by BMBF and DFG.

* grundmann@atom.uni-frankfurt.de

† a.kheifets@anu.edu.au

[1] B. Krässig, E. P. Kanter, S. H. Southworth, R. Guillemin, O. Hemmers, D. W. Lindle, R. Wehlitz, and N. L. S. Martin, Phys. Rev. Lett. **88**, 203002 (2002).

[2] F. Maulbetsch, and J. S. Briggs, J. Phys. B **28**, 551 (1995).

[3] O. Schwarzkopf, B. Krässig, J. Elmiger, and V. Schmidt, Phys. Rev. Lett. **70**, 3008 (1993).

[4] A. Knapp, A. Kheifets, I. Bray, Th. Weber, A. L. Landers, S. Schössler, T. Jahnke, J. Nickles, S. Kammer, O. Jagutzki, L. Ph. H. Schmidt, M. Schöffler, T. Osipov, M. H. Prior, H. Schmidt-Böcking, C. L. Cocke, and R. Dörner, J. Phys. B **38**, 615 (2005).

[5] R. Dörner, V. Mergel, O. Jagutzki, L. Spielberger, J. Ullrich, R. Moshammer, and H. Schmidt-Böcking, Phys. Rep. **330**, 95 (2000).

[6] J. Ullrich, R. Moshammer, A. Dorn, R. Dörner, L. Ph. H. Schmidt, and H. Schmidt-Böcking, Rep. Prog. Phys. **66**, 1463 (2003).

[7] T. Jahnke, Th. Weber, T. Osipov, O. Jagutzki L. Ph. H. Schmidt, C. L. Cocke, M. H. Prior, H. Schmidt-Böcking, and R. Dörner, J. Electron Spectrosc. Relat. Phenom. **141**, 229 (2004).

[8] J. Viefhaus, F. Scholz, S. Deinert, L. Glaser M. Ilchen, J. Seltmann, P. Walter, and F. Siewert, Nucl. Instr. and Methds. A **710**, 151 (2013).

[9] O. Jagutzki, J. Lapington, L. Worth, U. Spillman V. Mergel, and H. Schmidt-Böcking, Nucl. Instrum. Methods Phys. Res. A **477**, 256 (2002).

[10] O. Jagutzki, V. Mergel, K. Ullmann-Pfleger, L. Spielberger, U. Spillman R. Dörner, and H. Schmidt-Böcking, Nucl. Instrum. Methods Phys. Res. A **477**, 244 (2002).

[11] A. Knapp, A. S. Kheifets, I. Bray, Th. Weber A. L. Landers, S. Schössler, T. Jahnke, J. Nickles, S. Kammer, O. Jagutzki, L. Ph. H. Schmidt, T. Osipov, J. Rösch, M. H. Prior, H. Schmidt-Böcking, C. L. Cocke, and R. Dörner, Phys. Rev. Lett. **89**, 033004 (2002).

[12] A. Kheifets, J. Phys. B **34**, L247 (2001).

[13] J. H. McGuire, Electron Correlation and Dynamics in Atomic Collisions, Cambridge University Press (2005).

[14] M. Ya. Amusia, E. G. Drukarev, V. G. Gorshkov, and M. O. Kazachkov, J. Phys. B **8**, 1248 (1975).

[15] M. S. Schöffler, C. Stuck, M. Waitz, F. Trinter, T. Jahnke, U. Lenz, M. Jones, A. Belkacem, A. L. Landers, M. S. Pindzola, C. L. Cocke, J. Colgan, A. Kheifets, I. Bray, H. Schmidt-Böcking, R. Dörner, and Th. Weber, Phys. Rev. Lett. **111**, 013003 (2013).

[16] A. Y. Isotomin, N. L. Manakov, A. V. Meremianin, and A. F. Starace, Phys. Rev. A **71**, 052702 (2005).

[17] T. Suric, E. G. Drukarev, and R. H. Pratt, Phys. Rev. A. **67**, 022709 (2003).

[18] M. Y. Amusia, and E. G. Drukarev, J. Phys. B **36**, 2433 (2003).